ANALYSIS OF FIELD DATA AND SPATIAL METHODS FOR THE PARAMETRIZATION OF A SPATIAL DUFF CONSUMPTION MODEL

HUMBOLDT STATE UNIVERSITY

By

William Levi Gill

A Thesis

Presented to

The Faculty of Humboldt State University

In Partial Fulfillment

Of the Requirements for the Degree

Master of Science

In Environmental Systems: Mathematical Modeling

May, 2012

ANALYSIS OF FIELD DATA AND SPATIAL METHODS FOR THE PARAMETRIZATION OF A SPATIAL DUFF CONSUMPTION MODEL

HUMBOLDT STATE UNIVERSITY

By

William Levi Gill

Approved by the Master's Thesis Committee:

Dr. Christopher Dugaw, Major Professor	Date
Dr. Morgan Varner, Committee Member	Date
Dr. Borbala Mazzag, Committee Member	Date
Dr. Christopher Dugaw, Graduate Coordinator	Date
Dr. Jená Burges, Vice Provost & Graduate Dean	Date

ABSTRACT

ANALYSIS OF FIELD DATA AND SPATIAL METHODS FOR THE PARAMETRIZATION OF A SPATIAL DUFF CONSUMPTION MODEL

William Levi Gill

Field data collected from the consumption of organic forest soil (duff) by smoldering combustion are analyzed to determine the spatial patterns as input for a smoldering combustion model. Moisture, organic, and inorganic contents were measured at longleaf pines to detect patterns that could be used to explain the spatial patterns in post-burn consumption. The model takes these environmental predictors as input values and then outputs spatial consumption patterns. Methods are also developed to describe the two-dimensional spatial patterns of consumption created by the smoldering combustion. The spatial patterns revealed that smoldering combustion occurs most often at the base of a tree stem at the reintroduction of wildland fire in long-unburned forest. The data from the organic soil parameters were unable to completely predict this behavior, indicating that other factors might be involved. Duff depth was noted as being significantly higher at the areas of smoldering initiation indicating that understanding the soil characteristics of these deep duff mounds at the tree base will help predict smoldering patterns, and therefore deserve further research.

ACKNOWLEDGEMENTS

My sincerest gratitude to my committee Dr. Chris Dugaw, Dr. Bori Mazzag, and Dr. Morgan Varner for their constant guidance throughout this process. The hours they spent working through ideas and providing feedback was invaluable to the success of this work.

To the Wildland Fire Lab crew: Eamon Engber was always willing to answer questions with expertise in a field where I was just a novice. Erin Banwell provided me with the invaluable experience of visiting her field work out in Lake Tahoe. Jonathan Szecsei put in many hours entering data with me at a busy time of the semester, and I was grateful for his help.

I would further like to acknowledge the Joint Fire Science Program for funding the data collection on which this research is based.

To my fellow Math Grads, who made my time and experience through the program enjoyable. Kyle Falbo, Liz Arnold, Holly Perryman, and especially Amber Buntin were always willing to help me navigate the grad school waters. A special thanks to Michael Stobb for some timely m-files.

I am infinitely grateful to my family. To my parents Brad and Lisa, thank you for every sacrifice you made to train and educate me. To my in-laws Kevin, Beth, Bethany, Jonathan, and Hannah, thank you for all the encouragement and fun times we shared over these years of school.

Finally, to my dear wife Brianne. Thank you for every moment of joy we shared through this process. Thank you for your support, pushing me on whenever I needed encouragement. I have treasured these years in school with you. *Soli Deo Gloria.*

TABLE OF CONTENTS

LIST OF FIGURES

LIST OF TABLES

INTRODUCTION

Forest land managers and policy makers are faced with the goal of enacting fire policy that ensures both the safety of private and public lands, biodiversity, and ecological restoration (Dickinson and Ryan, 2010). Past strategies and policies to this end included fire suppression; however, current research has indicated that fire suppression was counteracting land management goals because of the accumulation of forest fuel loads, particularly with the increase of organic soil (often called "duff") (Hungerford et al., 1996; O'Brien et al., 2010; Dickinson and Ryan, 2010). While wildland fires are necessary for reducing fuel loads, contemporary re-introductions of wildland fire into long-unburned forests have resulted in greater severity, producing cascading ecological effects (Varner et al., 2005, 2007). Many of these impacts are positively correlated with the amount of organic soil consumed (Sandberg, 1980; Swezy and Agee, 1991; Hille and Stephens, 2005; Varner et al., 2007; Hood, 2010). Thus, it is important to be able to predict the window of conditions that enable the reduction of forest fuel loads without triggering these effects.

The forest floor consists of organic matter that overlies mineral soil. In long-unburned stands where organic matter has accumulated, the organic layer is composed of three horizons. The uppermost horizon (O_i) is the litter and consists of recently fallen and unaltered organic matter from trees and other vegetation such as twigs, leaves, and bark (Miyanishi, 2001; Varner et al., 2005). Beneath the litter is the fermentation horizon (O_e), where organic matter has begun to decompose yet is still distinguishable despite changes in color and structure. The lowermost horizon is called the humus (O_a) and consists of finely decomposed organic material that is no longer recognizable (Miyanishi, 2001). The fermentation and humus horizons are collectively referred to as "duff." Cellulose, hemicellulose, and lignin compose the primary chemical structure of duff, and a diverse array of other

chemicals determined by local vegetation are also contained within duff (Miyanishi, 2001). Additionally, the small particle sizes and dense packing of the decomposed material results in low oxygen contents, compromising the flammability of these fuels.

Forest fuels are consumed through the oxidation process of combustion. Fuels contain components that have lower molecular weights (e.g., fats, oils, waxes), which cause those components to volatilize at lower temperatures (Miyanishi, 2001). Flaming combustion is the result of rapid oxidation, characterized by the consumption of gaseous products created during the pyrolysis of the fuel, releasing large amounts of heat. Smoldering combustion, on the other hand, is a non-flaming combustion that relies on solid-phase oxidation to produce its heat and is a slower process, resulting in prolonged periods of raised temperatures. Although duff can be consumed by flaming combustion from a surface fire, it is more regularly consumed by smoldering combustion due to the high packing ratios (Frandsen, 1991; Miyanishi, 2001). It is common for flaming combustion of a passing surface fire to either initiate smoldering combustion in the underlying duff, or to ignite vectors (e.g., a pine cone or woody fuel) that will in turn ignite the duff (Fonda and Varner, 2005). Since moisture acts as a heat-sink, duff has to be dry enough for ignition, so in some cases enough heat must be generated to both dry and subsequently ignite the duff. Whereas a quick-passing surface fire may not be able to produce the necessary amount of heat to initiate smoldering combustion, often smoldering combustion of duff can continue long after a surface fire has passed, producing enough heat sustain the process up to hours and days (Rein, 2009), increasing the likelihood of secondary surface fires or excessive consumption of organic material.

A model to predict the behavior of smoldering duff fire was constructed by Holt (2008) as an extension of the previous research of Campbell et al. (1994) and Frandsen (1997). Holt's model is a spatial cellular automata model (Cronhjort, 2000) with discrete space and

time, and uses both deterministic and stochastic elements to simulate duff consumption. The model is designed to take input from various site conditions and then predict the spatial consumption patterns. Holt uses the equations by Campbell to determine the heat and moisture contents at each location, while relying on Frandsen's statistical equations to predict duff ignition of specific fuel types in order to avoid having to account for the numerous variables that would be impractical to collect from the field. As a result of combining these two methods, the model circumvents the issues of being too complicated or too site-specific for general use.

Holt's model is applied to a lattice, where each cell is given various parameters. Ideally, these values of each cell on the lattice would be determined from actual field data, although it is possible to apply estimates across the lattice as well. While some variables do not change during the combustion process until the cell is actually consumed (e.g., inorganic content), others variables are affected by the heat generated by neighboring cells in the combustion process (e.g., moisture content and temperature). Therefore, it is necessary to update some variables during each time step, while others can remain constant. Each cell in the lattice exists in one of three discrete combustion states (Figure 1): unburned, burning, or burned. It is assumed that a cell will not ignite unless a neighboring cell is already burning, and burn time of a cell is stochastically determined.

Since smoldering combustion typically occurs in the humus horizon with the fermentation horizon providing insulation (Varner et al., 2009), field values for humus horizon (O_a) are most applicable to the Holt model. Parameter input in the Holt model doesn't distinguish between horizons, so if there is a choice between measurements at the two horizons, values are taken from humus horizon.

The Holt model lacks field validation, therefore data from controlled field burns from northern Florida were collected for this purpose. Some of the field data could not be taken

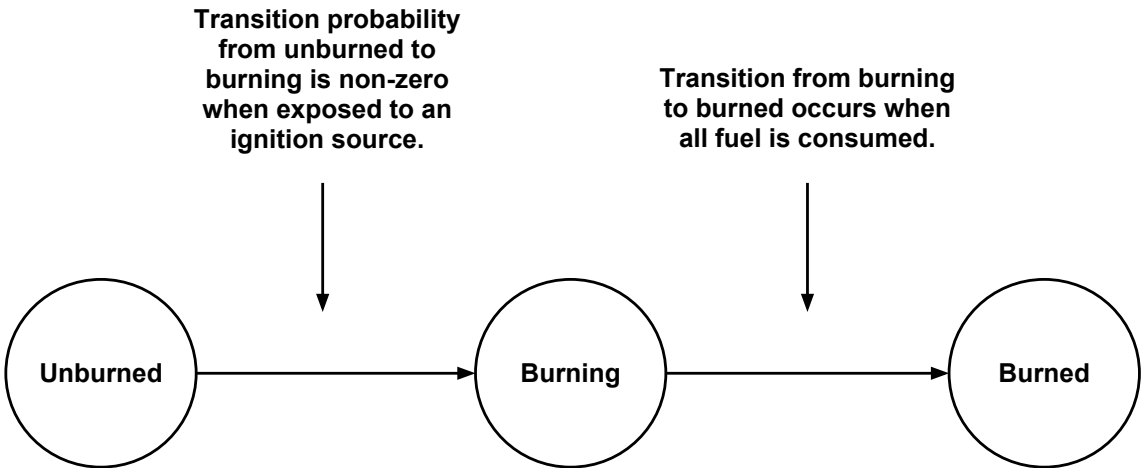

Figure 1: An individual cell in the Holt model can be in three combustion states: unburned, burning, and burned. The lattice starts almost entirely in the unburned state except for at predetermined locations that start in the burning state, which simulates ignition points. An unburned cell with no neighbors in the burn state has a zero probability of transitioning into the burning state. When it a unburned cell has a neighbor in the burning state, then the probability of ignition is determined by governing equations and Frandsen probabilities. The cell remains in a burning state for a randomly predetermined amount of time and then transitions and remains in the unburned state.

directly from a lattice without compromising the integrity of the experiment; instead samples were taken from other trees nearby the burn site (see Methods). Before the data can be used to validate the model, these estimates must be tested for their ability to predict the spatial patterns found on a lattice. Further, the post-burn spatial duff consumption patterns from the field must be compared to the output of the model. While there are numerous ways to measure spatial variability on a lattice with varying degrees of precision, this situation requires comparing spatial consumption patterns at two different scales. In order for the model to be stable it requires a scale significantly smaller than the scale of the field lattices.

This thesis has two primary objectives. The first is to develop and apply methods that can describe spatial patterns from the post-burn field data produced by smoldering combustion. To do this, a general metric is developed for this specific situation using pair approximations. One advantage of pair approximations is the ability to summarize the ecological behavior through clusters and edges (Iwasa, 2000). While various techniques exist for quantifying cluster and edge behavior, Iwasa (2000) demonstrates that often the most applicable technique can be developed individually for each modeling situation. For the Holt 2008 model two situations need to quantified: the clustering of burned cells and the spatial distribution of burn cells across the lattice. These two metrics are general enough to compare the output of the model and the field results without requiring a perfect match. These metrics can also be summarized with dimensionless proportions, which allows for comparisons to be made between results at different scales.

The second objective is to analyze the collected pre-burn field data to determine if they can explain the spatial patterns of post-burn combustion. However, before the pre-burn data can be applied it must be determined whether the samples taken at trees separate from the locations of the burns can be applied. This necessitates that the samples described an overarching pattern which can hold for all the trees within the stand where they were

collected; thus, statistical analysis is performed on the pre-burn data to find and described these patterns.

Literature Review

Many effects of duff consumption are a result of the length of time that smoldering persists. Frandsen (1991) reported durations of twelve hours at temperatures exceeding 300°C, while Hungerford et al. (1996) reported temperatures reaching a maximum of 600°C. Although flaming combustion results in higher temperatures, living tissue mortality occurs at only ca. 60°C (Byram, 1958). As the organic soil smolders, the underlying mineral soil can reach temperatures of 100°C to depths of 20cm (Varner et al., 2009). As a result, smoldering combustion often has been observed to kill or injure tree root tissues and dormant seeds. that reside in the mineral soil (Hungerford et al., 1996; Swezy and Agee, 1991; Zeleznik and Dickmann, 2004; O'Brien et al., 2010). Further, long-unburned stands often have an increased presence of embedded fine roots, which can be completely consumed along with the duff matrix (O'Brien et al., 2010). Duff consumption can also damage tree vascular tissues, especially when the duff accumulates against the base of the stem (Ryan and Frandsen, 1991). Although injury incurred during the smoldering combustion rarely results in immediate mortality, the stress from tree injury can leave the tree susceptible to future mortality (Varner et al., 2009; O'Brien et al., 2010).

Forest floor consumption also has a major impact on other ecosystem components. Because of the slow decomposition rate of duff, nutrients can become unavailable until a fire consumes the organic soil and makes the stored nutrients available (Miyanishi, 2001; Hungerford et al., 1996). The organic soil also contains dormant seeds capable of germinating only in a nutrient-rich ash seedbed, so their germination is dependent on forest floor

consumption (Hungerford et al., 1996). Smoldering combustion often results in patterned consumption leaving networks of unburned patches surrounded by large burned out depressions of exposed mineral soil, making accommodations for new vegetation (Miyanishi and Johnson, 2002; Knapp et al., 2007; Hungerford et al., 1996). While wildland fire is necessary for a variety of ecosystem processes, under adverse conditions it can cause excessive damage. Under prolonged heating, soil nutrients experience chemical changes, and dormant seeds can be killed (Hungerford et al., 1996; Hille and Stephens, 2005). Smoldering duff has been identified as a major source of noxious emissions and air pollutants (Sandberg, 1980; Frandsen, 1991), and with the urbanization into remote wildlands, air-quality issues have become increasingly important, narrowing the window of time that forest managers can safely burn (Knapp et al., 2007).

In order to understand and predict the process and results of smoldering combustion, mathematical modeling has been used. Modeling smoldering combustion of forest duff has been approached by two classical techniques: process-based and statistical modeling. The first approach is process-based (or deterministic) mathematical models that seek to create a set of equations based on the mechanisms of combustion (de Vries, 1963; Fahnestock and Hare, 1964; Dieckmann et al., 2000a; Dickinson and Ryan, 2010). The equations originate from theoretical research, while the variables are determined by empirical research. The equations are solved analytically or numerically. The advantage of a process-based model is that it can yield predictions across a variety of contexts (Dickinson and Ryan, 2010). Once a model has been validated against empirical data, it can be used in hypothesis testing to further the understanding of the mechanisms of combustion. The downside to this approach, however, is that process-based models can often become too complex, and risk either becoming difficult to interpret or too elaborate for practical use.

The second approach is statistical modeling, wherein a set of independent variables are

hypothesized to contribute to fire behavior or effects. Data are collected from experiments designed to test the hypothesis, and relationships are estimated. The advantage of the statistical approach is that it circumvents the need to understand the details and complexities of combustion and enables identification of the essential variables that drive the process. The primary disadvantage is that statistical models may only make predictions under situations in which they were developed, limiting their use to site-specific contexts. Creating a statistical model also presents the challenge of trying to create meaningful hypotheses that further scientific understanding, a consideration which has been overlooked (Miyanishi, 2001). In the past these two methods of modeling have been viewed as parallel methods of the same task. Recently a third approach has been developed that combines the advantages of both methods by creating deterministic equations for key parts of the processes, then using statistical equations to generalize site specific details.

There have been a progression of process based models that seek to understand how heat transfers during smoldering combustion. Most notably de Vries (1958) created a model that sought to predict the transport of heat and moisture in a porous media (e.g. duff), and has been used extensively as a framework for other models in soil physics. de Vries made an important distinction between liquid and vapor flux, because they can contribute uniquely to the transport of thermal energy, particularly when temperature gradients influence the flow of moisture vapor (de Vries, 1958). It was later shown by Cahill and Parlange (1998) by experimentation that vapor flux was a significant factor in thermal and moisture changes in the soil under heating, and that the model introduced by de Vries was able to reasonably capture this behavior. Campbell et al. (1994) developed a model based on a modification of the de Vries model in order to simulate soil heat and moisture transport during a surface fire. Campbell's model was validated against empirical data and was able to accurately predict temperatures but failed to accurately predict the moisture con-

tent (Hungerford et al., 1996; Holt, 2008). Campbell et al. (1995) suggested modifications of their original model that allowed for alternate mass flow assumptions that made better predictions of the moisture content.

Other types of smoldering combustion models have been proposed by Aston and Gill (1976) and Steward et al. (1990). These models reflect the general difficulties found in modeling smoldering combustion. The model by Aston and Gill (1976) was built and calibrated under the conditions of high temperatures, and as as result is only useful to similar situations limiting the scope of the model (Hungerford et al., 1996). In particular, Hungerford et al. (1996) found that outside those specific conditions, the model was unable to account for moisture content causing the model predictions to disagree with observed results. Steward et al. (1990) created a model of soil heat transfer to predict the depths at which temperatures could reach a level lethal to soil organisms. Since the objective was so specific, the model was one-dimensional and failed to account for moisture content, making it too simple for general application.

The statistical models by Frandsen (1987, 1991, 1997, 1998) have been seminal in understanding smoldering combustion. Many of Frandsen's models were created from empirical data, wherein he used peat as an equivalent for duff. Frandsen (1991) modeled the smoldering rate and mass loss as a function of variation in organic bulk density, moisture content, and inorganic content. Frandsen also worked to develop ignition probabilities of peat and a varieties of soils dependent only on moisture and inorganic content (Frandsen, 1987, 1991). Frandsen used logistic regression to predict a binary "burn/no burn" response. The advantage of this method is that it simplifies the process of making accurate predictions for the ignition of various soils since it uses only their moisture and inorganic content, rather than using deterministic equations that account for all of the details. Miyanishi and Johnson (2002) were able to use statistical models to show the significance of moisture in

the consumption process in field burns.

This research uses pair approximations to measure spatial variability that results from the complex spatial structures resulting from smoldering combustion. Pair approximations have been used extensively in spatially structured lattice models in the field of ecology (Iwasa (2000) provides a list of models). The original application of pair approximations in ecology was done by Matsuda et al. (1992) as an extension to the Lotka-Volterra model on a lattice. This method departed from the traditional mean-field approximation analysis used in spatial interaction models because the method assumed the homogeneity of the surroundings environment (Dieckmann et al., 2000b). Matsuda et al. (1992) instead developed a system of Ordinary Differential Equations to determine a state of a cell based on the state of its immediate neighbors, allowing for heterogeneity of the environment to effect the current state. The Holt (2008) model expands on this idea by using a system of Partial Differential Equations to determine, in part, the state of a cell from its neighbors, while also allowing for random effects.

METHODS

Field Data

Fuel samples were collected from experimental forest floor fires that occurred from 06 January to 06 April 2011 at the Ordway-Swisher Biological Station near Melrose (Putnam County), Florida (N 29° 40', W 81° 74'). The research site had not been burned for approximately 45 years and had accumulated a significant duff layer. The stand was composed of an overstory of longleaf pine (*pinus palustris*) with a midstory of oaks (*Quercus spp.*) (et al., 2012).

Thirty-three trees were randomly selected for burning, and of these burns 29 resulted in complete data sets that were usable for this research. There were notable accumulations of duff around the base of the tree stems (see Figure 2). At each tree a two-dimensional lattice of pins was arranged extending from the tree base. These pins were used to measure pre- and post- duff depths (see Figure 3). A perimeter was raked around the lattice down to the mineral soil as a buffer in order to contain the effects of fire to the lattice.

When the plots were burned, a fire was ignited at the far end of the plot away from the tree stem. The surface fire generally passed over the entire plot, consuming the litter. When the flaming front passed over there was opportunity for the initiation of smoldering combustion of underlying duff. Either the front itself generated sufficient heat to ignite the duff, or a fuel embedded in the litter (i.e. a vector: Varner et al. (2009)) ignited and initiated smoldering combustion in the underlying duff. The fire was allowed to burn until the end of the day before it was extinguished. The average burn time was five hours, ranging from 4.5 to 6 hours.

The organic bulk density ($\frac{kg}{m^3}$) and inorganic content ($\frac{kg}{kg}$) of the soil could not be sampled from the lattice without affecting the outcome of the burn. Instead seven trees were

Figure 2: A plot from the field site at Ordway before the lattice of pins was installed. The perimeter was raked down to the mineral soil to contain the fire on the plot. The accumulation of duff at the base of the stem is clearly seen as well as the embedded pine cones. Other embedded fuels found in other plots might include 10hr, 100hr, and 1000hr woody fuels.

randomly selected from the stand to measure these properties, and the results of these samples were then applied to the trees selected for burning. Each of these seven trees were sampled at points 15, 45, 90, and 135 cm along a row extending away from the tree stem (see Figure 4).

Since the samples were taken at neighboring trees, in order to apply them to either the burn lattice or the model input a relationship must be determined. It is assumed from the sampling method that this relationship would generally be linear, thus linear regression was applied. If a relationship existed that was non-linear then the linear regression would either fail or some type of pattern would emerge in the residuals. Three regression models were

considered for fitting the bulk density or inorganic content data:

$$\text{Model 1:} \quad y_1 = \beta_0 + \beta_1 \cdot \text{distance} + \beta_2 \cdot \text{tree} + \beta_3 \cdot \text{distance} : \text{tree},$$

$$\text{Model 2:} \quad y_2 = \beta_0 + \beta_1 \cdot \text{distance} + \beta_2 \cdot \text{tree},$$

$$\text{Model 3:} \quad y_3 = \beta_0 + \beta_1 \cdot \text{distance},$$

where y_i could represent either bulk density or inorganic content. The distances were 15, 45, 90, and 135 cm, correlating to the positions 1, 3, 6, and 9 respectively (see Figure 4). For each estimated coefficient $\beta_{0...}\beta_3$ a t-statistic was calculated and tested for significance ($\alpha = 0.05$), where the null hypothesis was that the value of the coefficient is equal to zero. The fourth term in Model 1 measures the interaction between each tree and distance, while Model 2 assumes instead that the relationship between consecutive points from the same tree is the same relationship for the other trees. Model 3 assumes that trees have no effect whatsoever. These models were compared using Akaike Weights, which are the probabilities of a model being the best model based on their AIC value (Stauffer, 2008). The model with the highest Akaike Weight was assumed to be the model that best explains the data.

Similar to the bulk density and inorganic content, the moisture content ($\%$) could not be sampled from the lattice of the burn plot. In this case, on the day of burn the moisture content of two neighboring trees were measured at their tree base and two meters from the base (see Figure 5). These moisture values would be applied to the plots being burned that day. If two trees were burned on the same day, the moisture contents from the neighboring trees would be applied to both. There were eighteen burn days, so thirty-six trees were measured for moisture content.

Because of the high variability of the moisture content of the two neighboring trees

(see Figure 11), these measurements could not be directly applied to the plot using averages. Instead the moisture contents were analyzed using Mixed Effects Linear Modeling (Stauffer, 2008). This method allows the data from all thirty-six sampled trees to be used in a regression since it accounts for errors produced both by within-stand variability and day of burn variability. The difference between the two measurements at each sampled tree were used as the response variable since taking the difference reduced two data points into a single measurement. The resulting equation was:

$$y = \beta_0 + \hat{b}_{\text{date}} + e \sim N(0, \sigma),$$

where β_0 is the intercept, and the response variable is y. If y >0, then the tree base had a higher moisture content than two meters from the tree base. The error produced by day of burn variability is given by $\hat{b}_{\text{date}}$, and the error produced by within-stand variability is given by e.

A graphical analysis was performed to study the relationship between moisture content of the two adjacent trees (on the day of burn) to post-fire consumption. For each burn the following figures were created: consumption versus the average moisture content of the adjacent trees at the tree base; consumption versus average moisture content two meters from the tree base; consumption versus average moisture contents of both the adjacent tree.

Spatial Analysis

Two aspects of the spatial distribution of duff consumption caused by smoldering combustion were measured. The first aspect was the pattern of consumption within regions at various distances from the tree stem, referred to as concentration. Since the model assumes that parameters experience changes horizontally but not vertically, the lattice columns were

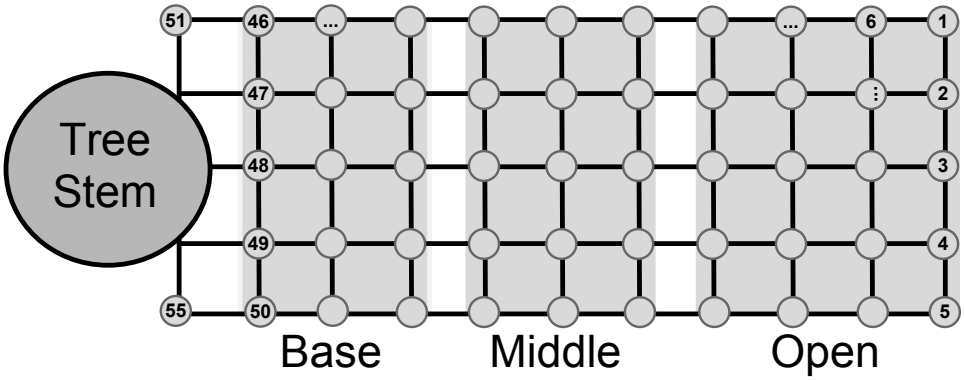

Figure 3: A 60 x 150 cm lattice was used for collecting the field data. There are forty cells (15 x 15 cm) and 55 lattice points corresponding to the location of each pin. Because the tree often intercepted some of the lattice points, the column of pins closest to the tree was disregarded for this study, leaving only 50 pins on a 5 x 10 grid. The lattice is divided into three sections: Base, Middle, and Open.

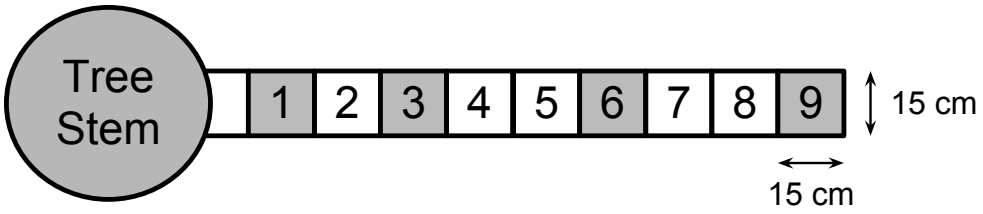

Figure 4: Seven trees within the study site were sampled from a 5 x 135 cm grid to measure both bulk density and inorganic content. In this case four edge pins are averaged to give a value for a cell.

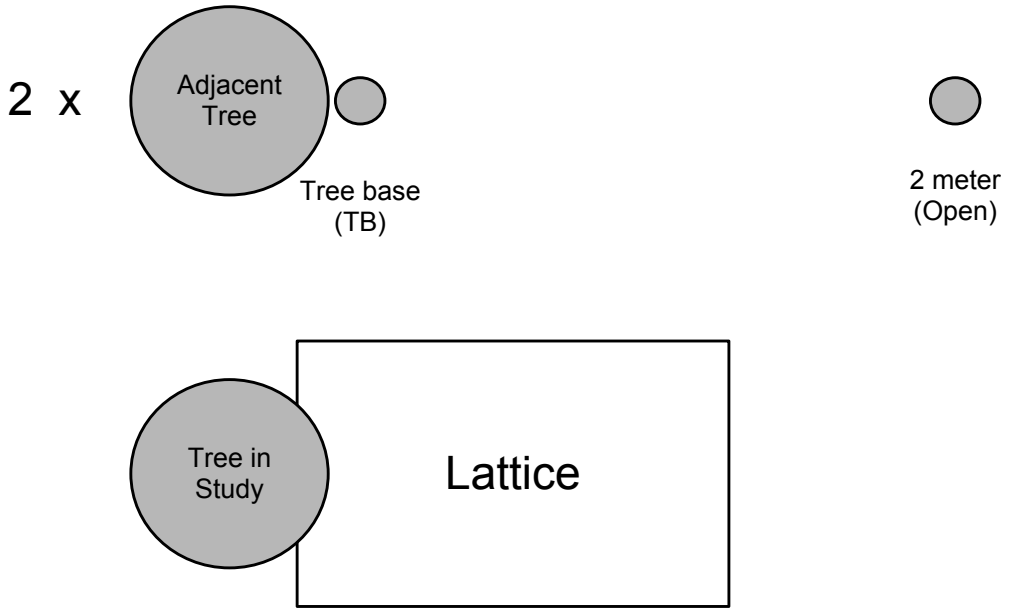

Figure 5: Moisture contents for each tree in the study was estimated from two adjacent trees on the day of the burn. Each adjacent trees were measured at the tree base (TB) and 2 meters from the tree base (Open). The Open position is 50 cm further from the tree stem than the furthest edge of the lattice.

categorized into three regions based on distance: Base, Middle, and Open, with the Base region being the closest to the tree stem (see Figure 3). The Base and Middle regions contained the same number of columns, but the Open region contained an extra column since the lattice could not be evenly divided into three regions.

Each point on the lattice was evaluated for duff consumption. There were two conditions used to to determine whether or not a point experienced any smoldering combustion. In the first method the point was considered "Burned" if any amount of duff reduction occurred, and "Unburned" otherwise (this method referred to as the 0% threshold). The second method was similar except a point was considered "Burned" if there was at least 5% of duff reduction. The selection of 5% as the second criterion came after observing the post-burn consumption data. Even with the use of an infrared camera which could track the consumption throughout the entire burn, it was not always clear whether the consumption was a result of the passing surface fire or from smoldering combustion. Increasing the criteria to 5%, however, could also remove any points that had just started smoldering combustion but were extinguished at the conclusion of the experiment. Thus the implementation of both methods helps ensure that the conclusions weren't based on false positives: if certain behaviors were consistent under both conditions, then this would infer stronger results.

The percent of points burned in the entire plot were calculated, as well as the proportion of points burned in each region. In order to determine whether or not a pattern of consumption was created by random chance or guided by some mechanism, a permutation test (Ramsey, 2001) with $\alpha = 0.05$ was performed under the null hypothesis that the observed distribution of the burned points among the regions was uniformly random, since under random conditions the distribution of consumed points within the entire plot would be uniform. Thus the expected distribution of consumed points within each region was

equal to the area of that region: namely,

$$[\text{Base, Middle, Open}] = [0.3, 0.3, 0.4].$$

For each burn the following Euclidean distance was calculated:

$$\sqrt{\sum (X_o - X_e)^2},$$

where X_o is the observed proportion of consumed points for a region and X_e is the expected distribution of consumed points for that region, summed over all the regions. To calculated the p-value, the data from the observation was scrambled 1000 times by random permutations, and the Euclidean distances were re-calculated. The p-value was given by the number of permutations that resulted in Euclidean distances greater or equal to the Euclidean distances created by the original observations, divided by the number of permutations (Ramsey, 2001). If null hypothesis was rejected, then the distribution was non-random, indicating that there was some mechanism driving the patterns.

The second aspect of spatial distribution of duff consumption was a measure of general patchiness, referred to as aggregation. The aggregation of burned points were evaluated using distributions of burned pairs (Dieckmann et al., 2000a) with von Neumann neighborhoods (i.e. up, down, right, left). To do this, all neighboring pairs were compared, and the number of burn/burn (bb), unburned/burned (ub), and unburned/unburned (uu) neighbors were counted (see Figure 6). Then the proportion of each were calculated:

$$\text{UU} = \frac{\text{Total Number of } uu \text{ pairs}}{\text{Total Number of Pairs}}$$

$$\text{UB} = \frac{\text{Total Number of } ub \text{ pairs}}{\text{Total Number of Pairs}}$$

$$\text{BB} = \frac{\text{Total Number of } bb \text{ pairs}}{\text{Total Number of Pairs}}$$

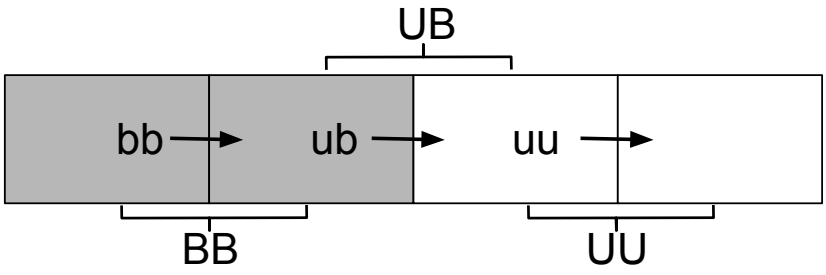

Figure 6: Examples of the pair-wise neighbors uu, ub, and bb. The proportion of each type of pair is indicated by UU, UB, and BB.

These proportions help describe the overall consumption patterns. If the consumption is aggregated together, as in a front or a large patch, then either UU and BB will be large - depending on the amount of consumption - and UB will be small. If however, the consumption didn't cluster into a front or patch, then both UU and BB would be lower while UB would be higher since there more edges are present.

To determine whether the aggregation was created randomly or by some mechanism, a permutation test was again performed (α=0.05), with the null hypothesis that the distribution of pairs arises from a uniform probability, given that the points are independent. If the distribution of pairs were random, then the expected distribution of UU, UB, and BB

would be:

$$\begin{bmatrix} \text{BB}_{\text{expected}} \\ \text{UB}_{\text{expected}} \\ \text{UU}_{\text{expected}} \end{bmatrix} = \begin{bmatrix} p^2 \\ 2p(1-p) \\ (1-p)^2 \end{bmatrix},$$

where, p is the proportion of burned pins in the lattice. The data set was scrambled 1000 times with random permutations, and the pairs were recalculated. The p-value was given by taking the number of number of permuted sets that resulted in a pair-wise distribution greater than or equal to the expected distance and dividing by the number of permuted data sets used. If the test rejected the null hypothesis, then the consumption pattern is more organized than random, indicating some type of mechanism guiding the aggregation.

RESULTS

Spatial Analysis at 0% threshold

When 0% of duff reduction was used to classify a pin as burned, the median of burned pins for all plots was 20% (see Tables 1, 2). The average distribution of burned pins throughout the regions was 51%, 23%, and 25% for the Base, Middle, and Open regions respectively. The distribution of burned cells amongst the three regions was significantly different than random ($p < 0.05$) in twelve of the twenty-nine plots, with those plots having an average consumption of 27% (median 30%). All twelve plots experienced a concentration of consumption near the tree base. The plots that did not have significant concentration of burned cells had an average consumption of 29% (median 14%).

The analysis of grouping by neighbor pair types resulted in the average distribution of 61%, 23%, and 16% of the unburned/unburned (UU), unburned/burned (UB), and burn/burn (BB) pairs, respectively. Clustering of the pairs was significant in fourteen of the twenty-nine plots, with those plots having an average consumption of 30% (median 31%). The plots that did not have significant concentration of burned cells had an average consumption of 26% (median 14%).

Spatial Analysis at 5% threshold

When 5% of duff reduction was used to classify a pin as burned, the median of burned pins for all plots was 20% (see Tables 3, 4). The average distribution of burned pins throughout the regions was 51%, 20%, and 22% for the Base, Middle, and Open regions respectively. The distribution of burned cells amongst the three regions was significantly different than random ($p < 0.05$), with those plots having an average consumption of 27% (median 26%). Of those thirteen plots, twelve experienced a concentration of the consumption near the tree

base. The plots that did not have a significant concentration had an average consumption of 21% (median 10%).

The analysis of grouping by neighbors resulted in the average distribution of 67%, 19%, and 14% of the unburned/unburned (UU), unburned/burned (UB), and burn/burn (BB) pairs respectively. The aggregation of the pairs was significant in eighteen of the twenty-nine plots, with those plots having an average consumption of 25% (median 25%). The plots that did not have significant aggregation had an average consumption of 23% (median 8%).

In seven cases (plots 12, 16, 18, 22, 24, 32, 34) the two methods disagreed about the occurrence of clustering. Plot 34 had concentration of consumption in regions but the test didn't detect any aggregation of pairs. Plots 12, 16, 18, 22, 24, 32, 34 had detected the aggregation of consumption by pairs but didn't detect a concentration of consumption in regions.

Organic Bulk Density

Two linear regression models were fitted to the bulk density of seven trees at distances of 15, 45, 90, and 135cm from tree stem (see Figure 7). Model 2 best explained the data (AIC weight = 0.95). Models 1 and 3 had AIC weights of 0.05 and 0.00 respectively. Therefore, of the models considered Model 2 best explains the data. Both the intercept and distance coefficients were statistically significant ($p < 0.01$). The multiple-R^2 value was 0.65, and the residual standard error was N(0,0.03). The residuals plotted against the fitted values resulted in a random dispersion about zero, with no apparent trend that would indicate a non-linear relationship exists among the data (see Figure 8).

						Ignitions		
Plot	Burned	Base	Middle	Open	p-val	Base	Middle	Open
1	0.34	0.76	0.06	0.18	<**0.01**	3	0	0
2	0.14	0.57	0.14	0.29	0.33	4	0	0
5	0.16	1.00	0.00	0.00	<**0.01**	7	0	0
6	0.36	0.67	0.17	0.17	<**0.01**	6	0	0
7	0.60	0.47	0.27	0.27	0.13	4	2	0
8	0.38	0.68	0.21	0.11	<**0.01**	n/a	n/a	n/a
9	0.04	0.00	1.00	0.00	0.18	4	2	0
10	0.12	1.00	0.00	0.00	<**0.01**	5	0	5
11	0.10	0.60	0.20	0.20	0.52	n/a	n/a	n/a
12	0.14	0.14	0.71	0.14	0.07	2	0	0
13	0.06	0.33	0.33	0.33	1.00	0	2	0
14	0.02	0.00	0.00	1.00	1.00	n/a	n/a	n/a
15	0.20	1.00	0.00	0.00	<**0.01**	5	0	0
16	0.16*	0.63	0.13	0.25	0.18	4	0	0
17	0.12	1.00	0.00	0.00	<**0.01**	n/a	n/a	n/a
18	0.18*	0.67	0.11	0.22	**0.05**	n/a	n/a	n/a
19	0.12	0.17	0.33	0.50	0.87	0	2	1
20	0.30	0.73	0.20	0.07	<**0.01**	4	1	2
22	0.32*	0.13	0.44	0.44	0.16	n/a	n/a	n/a
24	0.12	0.17	0.33	0.50	0.87	n/a	n/a	n/a
25	0.10	0.20	0.20	0.60	0.62	n/a	n/a	n/a
26	0.36	0.78	0.11	0.11	<**0.01**	n/a	n/a	n/a
27	0.42	0.67	0.19	0.14	<**0.01**	6	0	0
28	0.72	0.42	0.31	0.28	0.37	7	1	0
29	0.56	0.25	0.43	0.32	0.34	2	5	0
30	0.30	0.73	0.13	0.13	<**0.01**	7	1	1
32	0.66*	0.39	0.30	0.30	0.68	n/a	n/a	n/a
33	0.70	0.43	0.26	0.31	0.23	9	4	1
34	0.32	0.25	0.25	0.50	0.35	n/a	n/a	n/a
Mean	0.28	0.51	0.23	0.25				
Median	0.20	0.57	0.20	0.22				

Table 1: Analysis of spatial consumption patterns by concentration in regions at the 0% consumption threshold; that is, a pin is considered to be burned if there is any duff depth reduction at all. The Burned column indicates the percentage of pins within the lattice that were burned. The Base, Middle, and Open columns contain the distribution of those burned pins. If a p-value is less than 0.05, then the plot experienced a concentration of consumption within regions. The last three columns contain the number of points of ignition estimated from the infrared camera images. Consumption marked with '*', indicates that the methods to detect clustering disagreed.

Plot	Burned	UU, (expected)	UB, (expected)	BB, (expected)	p-val
1	0.34	0.54 (0.44)	0.25 (0.45)	0.21 (0.12)	<**0.01**
2	0.14	0.76 (0.74)	0.21 (0.24)	0.02 (0.02)	0.30
5	0.16	0.79 (0.71)	0.12 (0.27)	0.09 (0.03)	<**0.01**
6	0.36	0.48 (0.41)	0.33 (0.46)	0.19 (0.13)	**0.01**
7	0.60	0.21 (0.16)	0.39 (0.48)	0.40 (0.36)	0.09
8	0.38	0.46 (0.38)	0.32 (0.47)	0.22 (0.14)	<**0.01**
9	0.04	0.92 (0.92)	0.08 (0.08)	0.00 (0.00)	1.00
10	0.12	0.86 (0.77)	0.08 (0.21)	0.06 (0.01)	<**0.01**
11	0.10	0.81 (0.81)	0.18 (0.18)	0.01 (0.01)	1.00
12	0.14	0.71 (0.74)	0.28 (0.24)	0.01 (0.02)	0.14
13	0.06	0.89 (0.88)	0.11 (0.11)	0.00 (0.00)	0.66
14	0.02	0.95 (0.96)	0.05 (0.04)	0.00 (0.00)	0.56
15	0.20	0.79 (0.64)	0.06 (0.32)	0.15 (0.04)	<**0.01**
16	0.16*	0.75 (0.71)	0.20 (0.27)	0.05 (0.03)	**0.04**
17	0.12	0.85 (0.77)	0.08 (0.21)	0.07 (0.01)	<**0.01**
18	0.18*	0.72 (0.67)	0.24 (0.30)	0.05 (0.03)	0.08
19	0.12	0.75 (0.77)	0.24 (0.21)	0.01 (0.01)	0.36
20	0.30	0.61 (0.49)	0.20 (0.42)	0.19 (0.09)	<**0.01**
22	0.32*	0.53 (0.46)	0.29 (0.44)	0.18 (0.10)	<**0.01**
24	0.12	0.79 (0.77)	0.18 (0.21)	0.04 (0.01)	0.27
25	0.10	0.82 (0.81)	0.16 (0.18)	0.01 (0.01)	0.63
26	0.36	0.52 (0.41)	0.25 (0.46)	0.24 (0.13)	<**0.01**
27	0.42	0.45 (0.34)	0.26 (0.49)	0.29 (0.18)	<**0.01**
28	0.72	0.09 (0.08)	0.38 (0.40)	0.53 (0.52)	0.62
29	0.56	0.20 (0.19)	0.44 (0.49)	0.36 (0.31)	0.25
30	0.30	0.58 (0.49)	0.26 (0.42)	0.16 (0.09)	<**0.01**
32	0.66*	0.18 (0.12)	0.32 (0.45)	0.51 (0.44)	**0.02**
33	0.70	0.15 (0.09)	0.34 (0.42)	0.51 (0.49)	0.07
34	0.32	0.44 (0.46)	0.49 (0.44)	0.07 (0.10)	0.24
Mean	0.28	0.61	0.23	0.16	
Median	0.20	0.71	0.24	0.09	

Table 2: Analysis of spatial consumption patterns by pairs at the 0% consumption threshold; that is, a pin is considered to be burned if there is any duff depth reduction at all. The Burned column indicates the percentage of pins within the lattice that were burned. The next three columns show the proportion of total number of pairs that were classified as UU (unburned/unburned), UB (unburned/burned), and BB (burned/burned) alongside in parenthesis the expected proportion of these pairs within the plot. The expected values are calculated assuming a binary distribution. If a p-value is less than 0.05, then an aggregation of pairs occurred. Consumption marked with '*', indicates that the methods to detect clustering disagreed.

						Ignitions		
Plot	Burned	Base	Middle	Open	p-val	Base	Middle	Open
1	0.30	0.87	0.00	0.13	<**0.01**	3	0	0
2	0.08	0.75	0.25	0.00	0.08	4	0	0
5	0.12	1.00	0.00	0.00	<**0.01**	7	0	0
6	0.32	0.75	0.13	0.13	<**0.01**	6	0	0
7	0.48	0.58	0.25	0.17	<**0.01**	4	2	0
8	0.34	0.76	0.18	0.06	<**0.01**	n/a	n/a	n/a
9	0.00	0.00	0.00	0.00	1.00	4	2	0
10	0.12	1.00	0.00	0.00	<**0.01**	5	0	5
11	0.08	0.75	0.00	0.25	0.18	n/a	n/a	n/a
12	0.08*	0.00	0.75	0.25	0.18	2	0	0
13	0.04	0.00	0.50	0.50	1.00	0	2	0
14	0.00	0.00	0.00	0.00	1.00	n/a	n/a	n/a
15	0.20	1.00	0.00	0.00	<**0.01**	5	0	0
16	0.12*	0.67	0.17	0.17	0.22	4	0	0
17	0.12	1.00	0.00	0.00	<**0.01**	n/a	n/a	n/a
18	0.12*	0.50	0.17	0.33	0.65	n/a	n/a	n/a
19	0.04	0.00	0.50	0.50	1.00	0	2	1
20	0.24	0.83	0.08	0.08	<**0.01**	4	1	2
22	0.26*	0.15	0.38	0.46	0.43	n/a	n/a	n/a
24	0.10*	0.00	0.40	0.60	0.38	n/a	n/a	n/a
25	0.10	0.20	0.20	0.60	0.62	n/a	n/a	n/a
26	0.34	0.76	0.12	0.12	<**0.01**	n/a	n/a	n/a
27	0.40	0.70	0.20	0.10	<**0.01**	6	0	0
28	0.66	0.45	0.24	0.30	0.12	7	1	0
29	0.48	0.29	0.38	0.33	0.82	2	5	0
30	0.26	0.85	0.08	0.08	<**0.01**	7	1	1
32	0.54*	0.48	0.22	0.30	0.09	n/a	n/a	n/a
33	0.62	0.45	0.23	0.32	0.15	9	4	1
34	0.22*	0.00	0.36	0.64	0.03	n/a	n/a	n/a
Mean	0.23	0.51	0.20	0.22				
Median	0.20	0.58	0.18	0.17				

Table 3: Analysis of spatial consumption patterns by concentration in regions at the 5% consumption threshold. The Burned column indicates the percentage of pins within the lattice that were burned. The Base, Middle, and Open columns contain the distribution of those burned pins. If a p-value is less than 0.05, then the plot experienced a concentration of consumption in a region. The last three columns contain the number of points of ignition estimated from the infrared camera images. Consumption marked with '*', indicates that the methods to detect clustering disagreed.

Plot	Burned	UU, (expected)	UB, (expected)	BB, (expected)	p-val
1	0.30	0.64 (0.49)	0.15 (0.42)	0.21 (0.09)	<**0.01**
2	0.08	0.86 (0.85)	0.13 (0.15)	0.01 (0.01)	0.33
5	0.12	0.84 (0.77)	0.09 (0.21)	0.07 (0.01)	<**0.01**
6	0.32	0.56 (0.46)	0.25 (0.44)	0.19 (0.10)	<**0.01**
7	0.48	0.36 (0.27)	0.31 (0.50)	0.33 (0.23)	<**0.01**
8	0.34	0.54 (0.44)	0.24 (0.45)	0.22 (0.12)	<**0.01**
9	0.00	1.00 (1.00)	0.00 (0.00)	0.00 (0.00)	1.00
10	0.12	0.86 (0.77)	0.08 (0.21)	0.06 (0.01)	<**0.01**
11	0.08	0.86 (0.85)	0.13 (0.15)	0.01 (0.01)	0.33
12	0.08*	0.81 (0.85)	0.19 (0.15)	0.00 (0.01)	**0.04**
13	0.04	0.93 (0.92)	0.07 (0.08)	0.00 (0.00)	0.59
14	0.00	1.00 (1.00)	0.00 (0.00)	0.00 (0.00)	1.00
15	0.20	0.79 (0.64)	0.06 (0.32)	0.15 (0.04)	<**0.01**
16	0.12*	0.82 (0.77)	0.14 (0.21)	0.04 (0.01)	0.01
17	0.12	0.85 (0.77)	0.08 (0.21)	0.07 (0.01)	<**0.01**
18	0.12*	0.81 (0.77)	0.16 (0.21)	0.02 (0.01)	**0.05**
19	0.04	0.92 (0.92)	0.08 (0.08)	0.00 (0.00)	1.00
20	0.24	0.71 (0.58)	0.14 (0.36)	0.15 (0.06)	<**0.01**
22	0.26*	0.59 (0.55)	0.29 (0.38)	0.12 (0.07)	**0.04**
24	0.10*	0.84 (0.81)	0.13 (0.18)	0.04 (0.01)	**0.03**
25	0.10	0.82 (0.81)	0.16 (0.18)	0.01 (0.01)	0.61
26	0.34	0.53 (0.44)	0.27 (0.45)	0.20 (0.12)	<**0.01**
27	0.40	0.48 (0.36)	0.22 (0.48)	0.29 (0.16)	**0.00**
28	0.66	0.15 (0.12)	0.39 (0.45)	0.46 (0.44)	0.23
29	0.48	0.27 (0.27)	0.44 (0.50)	0.29 (0.23)	0.19
30	0.26	0.65 (0.55)	0.19 (0.38)	0.16 (0.07)	<**0.01**
32	0.54*	0.29 (0.21)	0.33 (0.50)	0.38 (0.29)	**0.01**
33	0.62	0.18 (0.14)	0.42 (0.47)	0.40 (0.38)	0.36
34	0.22*	0.59 (0.61)	0.38 (0.34)	0.04 (0.05)	0.49
Mean	0.23	0.67	0.19	0.14	
Median	0.20	0.79	0.16	0.07	

Table 4: Analysis of spatial consumption patterns by the aggregation of pairs at the 5% consumption threshold. The Burned column indicates the percentage of pins within the lattice that were burned. The next three columns show the proportion of total number of pairs that were classified as UU (unburned/unburned), UB (unburned/burned), and BB (burned/burned) alongside in parenthesis the expected proportion of these pairs within the plot. The expected values are calculated assuming a binary distribution. If a p-value is less than 0.05, then an aggregation of pairs occurred. Consumption marked with '*', indicates that the methods to detect clustering disagreed.

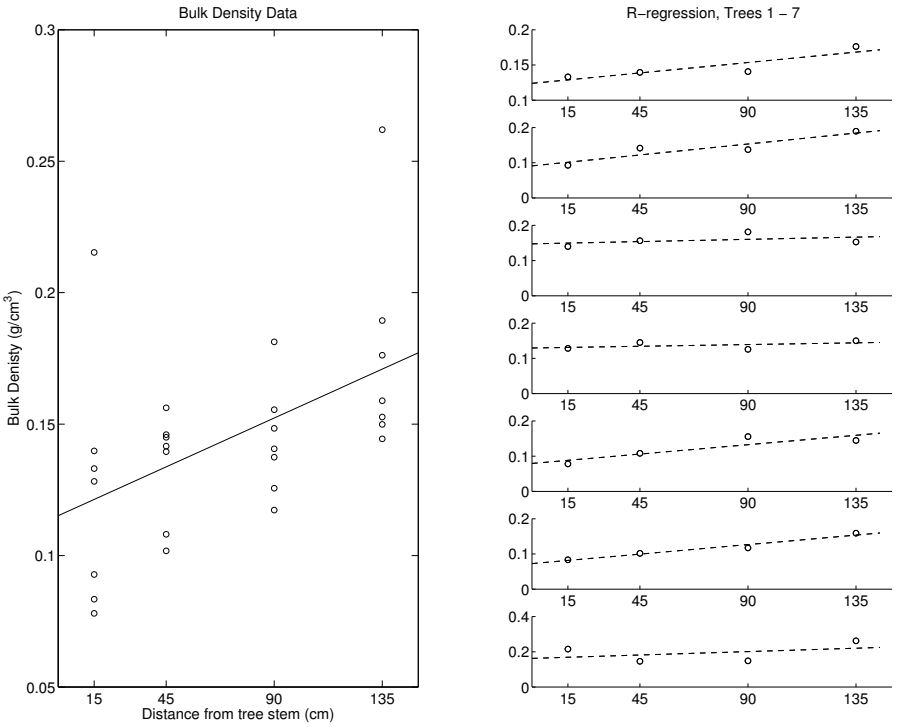

Figure 7: The plot on the left shows Model 2 plotted with all the Organic Bulk Density (g/cm^3) data collected from seven trees within the study site at 15, 45, 90, and 135cm from the base of the tree. On the right, Model 1 is plotted with the interactions for each individual tree along with the data from that tree.

Inorganic Content

Two linear regression models were fitted to the inorganic content of six trees at distances of 15, 45, 90, and 135cm from tree stem (see Figure 9). Model 1 best explained the data (AIC weight = 1.00). Models 2 and 3 had AIC weights of 0. Therefore of the models considered, Model 1 explained the data best. The coefficient for the intercept was not significant ($p = 0.28$), while the coefficient for the distance coefficient was ($p < 0.01$). Trees 4, 5, and 6 had statistically significant coefficients for the interaction terms. The multiple-R^2 value was 0.88 and the residual standard error was $N(0, 2.58)$. The residuals

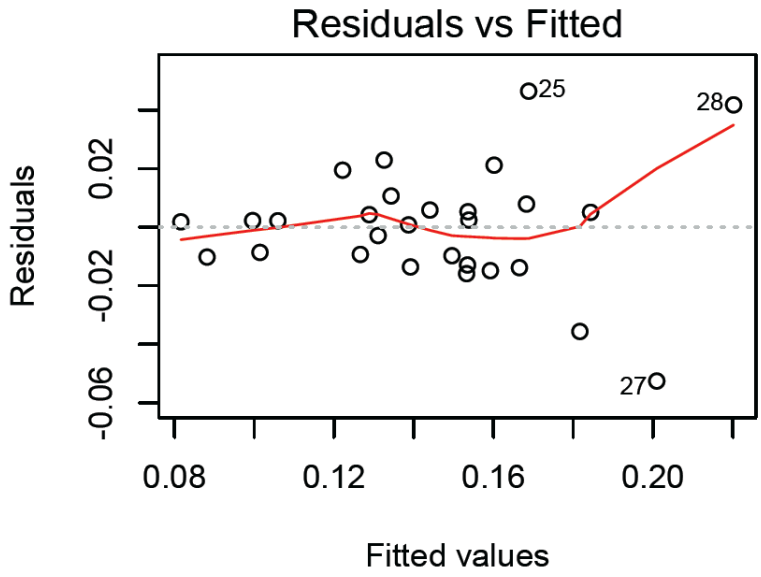

Figure 8: Residuals plotted with the fitted values of the linear regression Model 2 analyzing the bulk density.

plotted against the fitted values resulted in a random dispersion about zero, with no apparent trend that would indicate a non-linear relationship exists (see Figure 10).

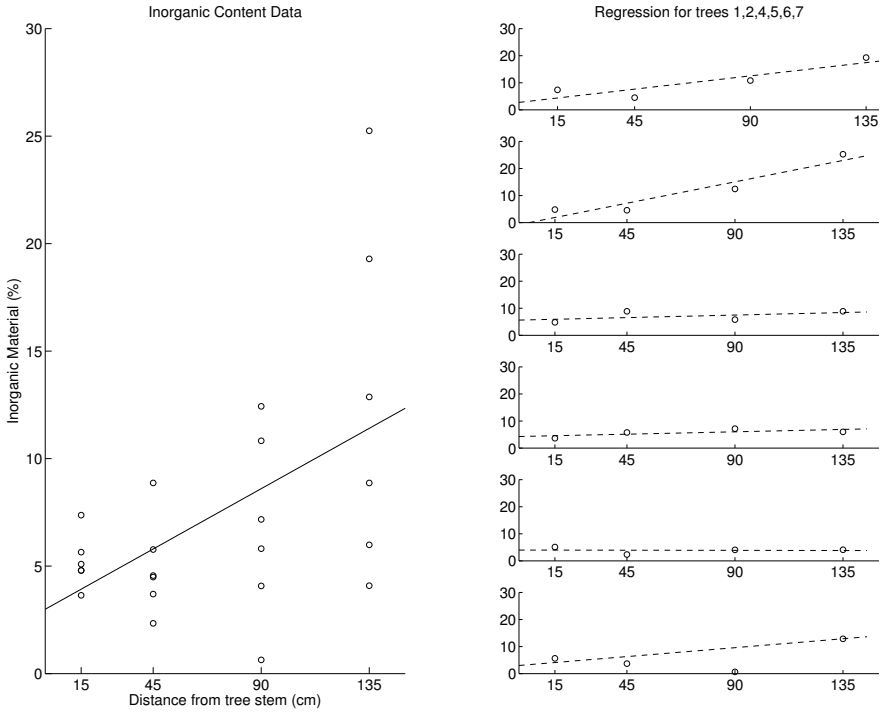

Figure 9: The plot on the left shows Model 2 plotted with all the Inorganic Material (%) data collected from six trees within the study site at 15, 45, 90, and 135cm from the base of the tree (tree3 was thrown out because of missing data). On the right, Model 1 is plotted with the interactions for each individual tree along with the data from that tree.

Moisture Content

The linear regression with mixed effects for the moisture data resulted in an intercept coefficient estimate of $\beta_0 = -0.69(\pm\ 2.90)$. No differences in the moisture content were detected between fuels at the base of the tree and two meters away $(p = 0.81)$. The error resulting from the day of burn variation was $\hat{b}_{\text{Date}} = N(0, 0.004)$, whereas the error for the within-stand variation was much greater at $e = N(0, 17.42)$.

Fuel moisture contents from the two adjacent trees were compared to the amount of consumption at the respective plots (see Figure 11). These comparisons include the average

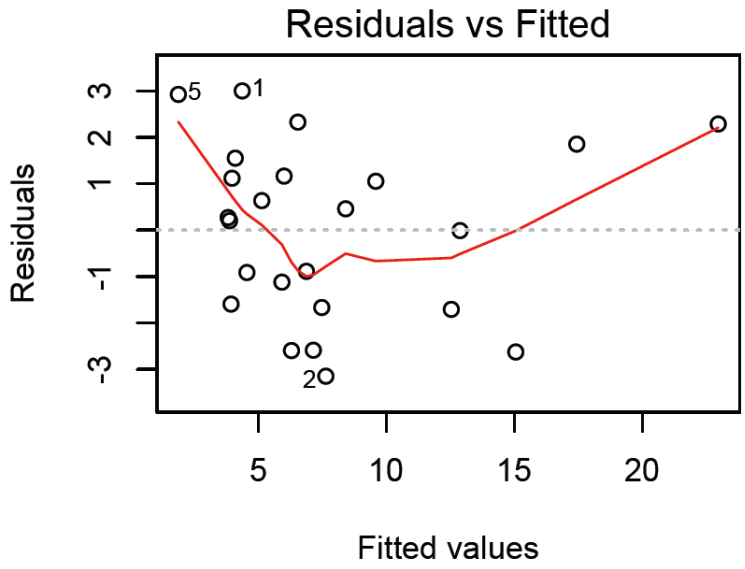

Figure 10: Residuals plotted with the fitted values of the linear regression Model 1 analyzing the inorganic content.

moisture content of the adjacent trees, the average moisture contents at the tree base, and average moisture contents two meters from the base.

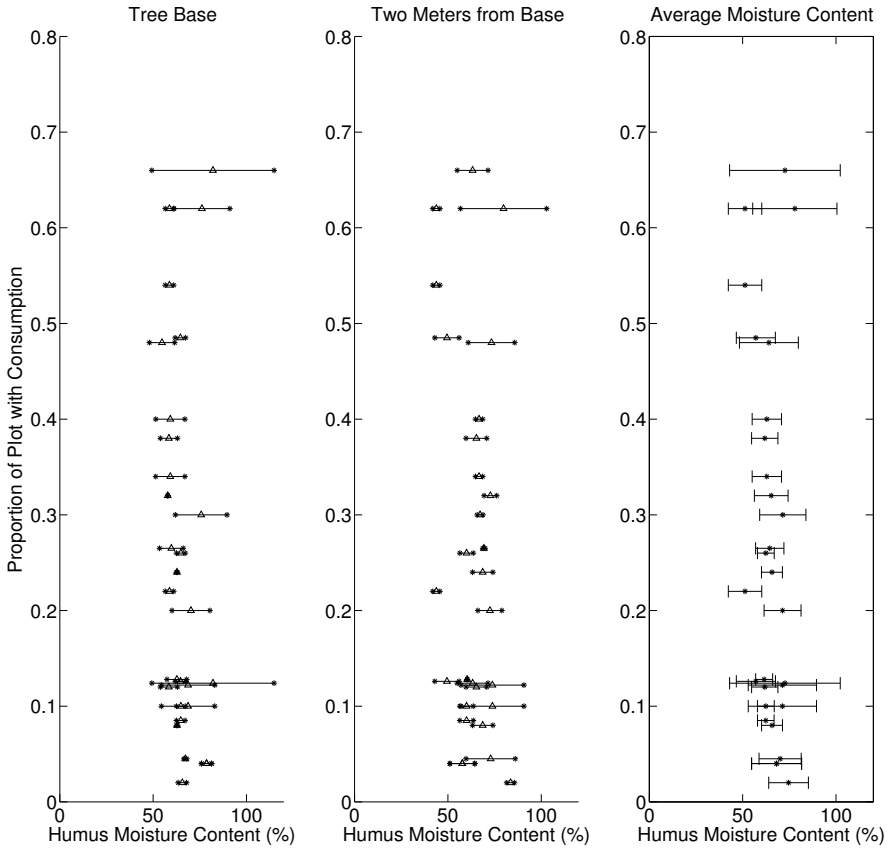

Figure 11: The moisture content of the sampled trees are plotted with the proportion of the plot that experienced consumption. The consumption is based on at least 5% reduction of the duff. The first two plots represent the moisture content of the two sampled trees on the day of burn at the indicated position. The actual data values of the locations are given as '*' and the average of the two values are given as '△'. The third plot is the average of the moisture content of the two trees. The error bars are one standard deviation from the mean.

DISCUSSION

Analysis of the spatial patterns created by the smoldering combustion revealed that the consumption was most often concentrated near bases, and of the ten burns for which this didn't occur, seven of them had a minimal consumption. It is notable that for all burns, the surface fire was ignited at the end of the plot farthest from the tree base, so in order for these patterns to occur, the surface fire had to pass over the entire plot before initiating smoldering combustion at the base of the tree without initiating many points of sustained smoldering combustion in previously burned regions (Miyanishi, 2001). This pattern indicates that there is some unique condition at the tree base that lends itself to smoldering combustion more readily than the forest floor away from the tree.

Frandsen (1997) demonstrated that bulk density, inorganic and moisture contents of duff could be used to determine the probability of ignition of duff. The lower these soil properties are the more likely duff ignition, therefore it is expect that the soil near the tree base would have lower values. Yet this pattern cannot be supported by the field burn data. In the case of the inorganic content, no relationship was found that related the inorganic content to the distance from the tree, even though visually the data seemed to indicate a slight linear increase. On the other hand, there was a consistent positive linear relationship between the distance from tree stem and organic bulk density. However, in both cases the sample sizes were insufficient to warrant a strong inference. Future work investigations of these trends should be prioritized.

Similarly, moisture content analysis relied on a small sample size, and the ability of these limited samples to make predictions is further exacerbated by the large measured variability. Figure 11 indicates that there is no correlation between the sample moisture contents and the amount of consumption at the neighboring plot. Again, the small sample

size prevents a strong inference especially considering the variability of moisture caused by weather patterns both on and preceding the day of burn.

There was a discrepancy between the probability of ignition predicted by the Frandsen (1997) equations and the field burning. Figure 12 is adapted from Frandsen's 1997 research, and it determines the 50% ignition probability of duff at various parameter values. The coefficients used were derived from lab burns of southern pine duff (Frandsen, 1997), and the average bulk density values were taken from the current field data. According to this probability, the range of values for moisture and inorganic contents were significantly low enough that the duff in all regions was expected to ignite. Yet not only was the majority of the consumption often concentrated at one side, the average consumption overall was low (see Tables 1, 3). The disparity cannot be dismissed as the inability of the data to predict the spatial patterns, regardless of the spatial patterns since those patterns would likely fall within that same range.

One explanation for the discrepancy could be the result of using the Frandsen (1997) ignition probability equation in the wrong context. First, Frandsen used a heated coil to ensure duff ignition. Thus the use of the Frandsen probability presumes that there is an appropriate amount of heat transfer to the duff to initiate the smoldering combustion, provided the soil conditions were conducive to burning. It is only under these conditions, then, that the Frandsen (1997) probability equation will give accurate prediction of field results. Second, the coefficients used from Frandsen (1997) are species-specific, and therefore the choice of coefficients may not have been appropriate for the composition of the stand in northern Florida. To remedy this, lab burns would have to be performed with samples take from each new location, and using methods described in Frandsen (1997), calculate the appropriate coefficients for this species. If this is the solution, then building a large database of coefficients for different species will allow the Holt (2008) model to be used in a wider

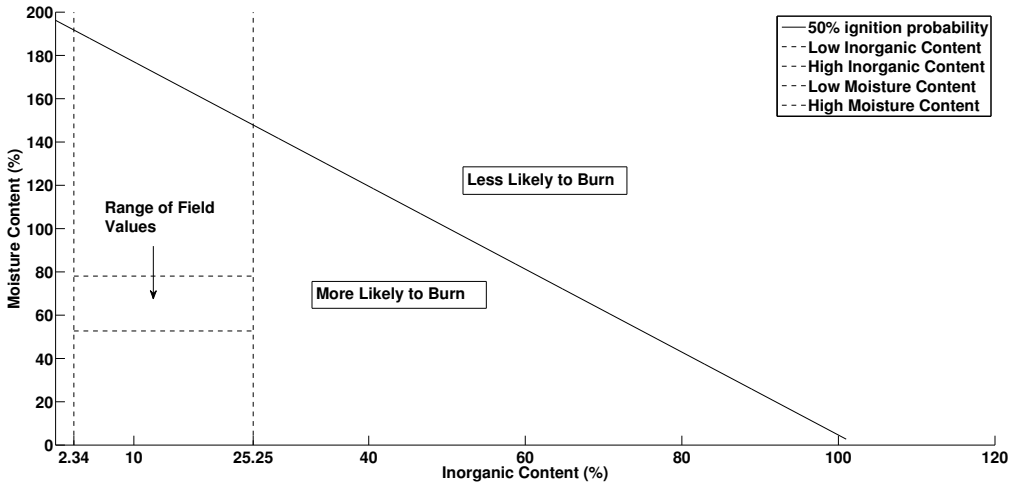

Figure 12: The probability of ignition for Southern pine duff (Frandsen, 1997). The solid line represents the fifty-percent chance of ignition. Coordinates above the line are less likely to burn, and coordinates below are more likely. The dotted lines indicate the lowest and highest values of inorganic content collect from the field. The circles correspond to the moisture contents measured in the studied.

set of contexts since it uses these equations, in part, to determine the ignition of the cells at each time step; otherwise, using the equations derived by Frandsen in this context may need to be re-evaluated.

Another option is that there may be other factors involved in duff ignition that aren't accounted for in Frandsen (1997). One soil characteristic that noticeably different at the base of the tree was duff depth. At each plot the duff depth was greatest at the tree base, often with a sharp increase creating a mound of duff (see Figure 13), as has been observed in many studies (Ryan and Frandsen, 1991; Garlough and Keyes, 2011). While the soil parameters may not be significantly different at the mound compared to the plot, it could be that the slope exposing fuel to more oxygen inflow or the amount of fuel may create ideal conditions to initiate the combustion. Future research should focus on the drivers of basal ignition.

The implication of the significance of duff depth in the Holt (2008) model remains to be determined. In the current modeling schema, the initial points of ignition of smoldering combustion are pre-determined. The Holt (2008) model does not make predictions as to which locations the flaming front will initiate the smoldering combustion, but assumes that the process has already begun. Therefore, if duff depth or slope only affects the initial ignition from the surface fire, no changes will be required of the current model. If, however, duff is more likely to burn because of basal slope or depth, then this will need to be incorporated more explicitly in the ignition probabilities used in the Holt (2008) model.

The reintroduction of fire into a long-unburned forest resulted in the smoldering combustion concentrating around the base of the tree stem. This demonstrates the need to understand and predict the process of smoldering combustion at this particular location. Garlough and Keyes (2011) has stressed the importance of understanding these duff mounds as a unique fuel type, but notes a current paucity of research on this topic. In her research, Garlough demonstrated that bulk density and inorganic content were not significant in predicting consumption at the duff mound, whereas moisture content was a major factor. Of all the parameter estimates of this current data set, moisture was the most variable, both from difference due to weather from day of burn as well as natural variation in the stand, so there could have been some type of interaction of moisture at these mounds that would have better explained these results.

In total, this research indicates that as the process of duff consumption is modeled, understanding the behavior at the tree base is paramount. Not only has the correlation between duff consumption at the tree base and tree mortality been emphasized due to the effects of the fire on the tree (e.g., Ryan and Frandsen (1991); Swezy and Agee (1991)), but it is now clear that this is also the primary location for the initiation of smoldering combustion. Modeling this process to predict the outcomes and effects will be necessary

for the implementation land management strategies in long-unburned forests.

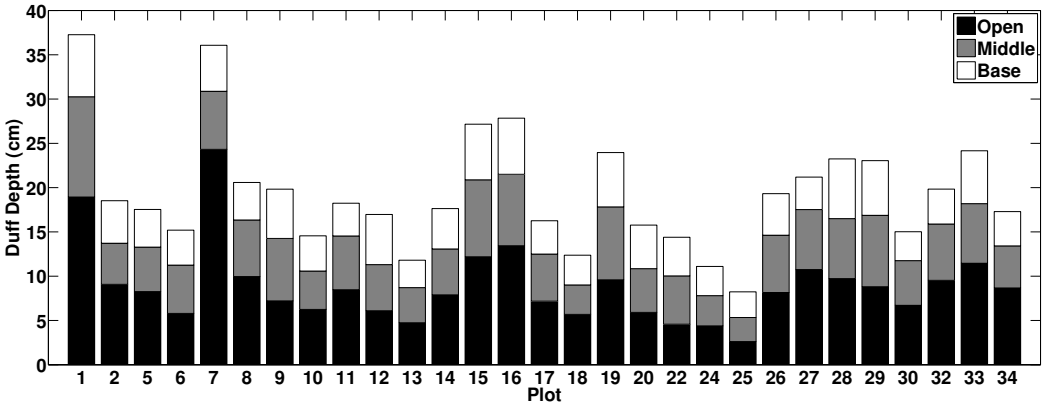

Figure 13: Average duff depths by region at each plot.

BIBLIOGRAPHY

Aston, A. R. and A. M. Gill. 1976. Coupled soil moisture, heat and water vapour transfer under simulated fire conditions. *Australia Journal of Soil Research*, **14**:55–66.

Byram, G. 1958. Some basic thermal processes controlling the effect of fire on living vegetation. Tech. rep., USDA Forest Service Note SE-114. Southeastern Forest Experiment Station, New Orleans.

Cahill, A. T. and M. B. Parlange. 1998. On water vapor transport in field soils. *Water Resources Research*, **34**:731–739.

Campbell, G. S., J. D. Jungbauer, W. R. Bidlake, and R. D. Hungerford. 1994. Predicting the effect of temperature on soil thermal conductivity. *Soil Science*, **158**:307–313.

Campbell, G. S., J. D. Jungbauer, K. L. Bristow, and R. D. Hungerford. 1995. Soil temperature and water content beneath a surface fire. *Soil Science*, **159**:363–374.

Cronhjort, M. 2000. The interplay between reaction and diffusion. In J. M. U. Dieckmann, R. Law, ed., *The Geometry of Ecological Interactions: Simplifying Spatial Complexity*, chap. 9, pp. 151–170. Cambridge University Press.

de Vries, D. A. 1958. Simultaneous transfer of heat and moisture in porous media. *Trans. Am. Geophys Union*, **39**:909–916.

de Vries, D. A. 1963. Thermal properties of soils. In *Physics of Plant Environment*, pp. 210–235. North Holland Publishing Co., Amsterdam.

Dickinson, M. and K. C. Ryan. 2010. Introduction: Strengthening the foundation of wildland fire effects prediction for research and management. *Fire Ecology*, **6**(1).

Dieckmann, U., R. Law, and J. Metz, eds. 2000a. *The Geometry of Ecological Interactions: Simplifying Spatial Complexity*. Cambridge University Press.

Dieckmann, U., R. Law, and J. Metz, eds. 2000b. *The Geometry of Ecological Interactions: Simplifying Spatial Complexity*. Cambridge University Press.

et al., E. 2012. Utility of an instantaneous moisture meter for duff moisture prediction in long-unburned longleaf pine forests.

Fahnestock, G. and R. Hare. 1964. Heating of tree trunks in surface fires. *Journal of Forestry*, **62**(11):799–805.

Fonda, R. and J. M. Varner. 2005. Burning characteristics of cones from eight pine species. *Northwest Science*, (78):322–333.

Frandsen, W. H. 1987. The influence of moisture and mineral soil on the combustion limits of smoldering forest duff. *Canadian Journal of Forest Research*, **17**:1540–1544.

Frandsen, W. H. 1991. Burning rate of smoldering peat. *Northwest Science*, **65**:166–172.

Frandsen, W. H. 1997. Ignition probability of organic soils. *Canadian Journal of Forest Research*, **27**:1471–1477.

Garlough, E. C. and C. R. Keyes. 2011. Influences of moisture content, mineral content, and bulk density on smouldering combustion of ponderosa pine duff mounds. *International Journal of Wildland Fire*, **20**:589–596.

Hille, M. G. and S. L. Stephens. 2005. Mixed conifer forest duff consumption during prescribed fires: Tree crown impacts. *Forest Science*, **51**:417–424.

Holt, B. V. 2008. *A Stochastic Spatial Model for the Consumption of Organic Forest Soils in a Smoldering Ground Fire*. Master's thesis, Humboldt State University.

Hood, S. M. 2010. Mitigating old tree mortality in long-unburned, fire-dependent forests: A synthesis. General Technical Report RMRS-GTR-238, United States Department of Agriculture.

Hungerford, R. D., W. H. Frandsen, and K. C. Ryan. 1996. Heat transfer into the duff and organic soil. Tech. Rep. FWS ref. no.14-48-0009-92-962 DCN 98210-2-3927, U.S Fish and Wildlife Service and U.S. Forest Service.

Iwasa, Y. 2000. *The Geometry of Ecological Interactions: Simplifying Spatial Complexity*, chap. 13, pp. 227–251. Cambridge University Press.

Knapp, E., D. Schwilk, J. Kane, and J. Keeley. 2007. Role of burning season on initial understory vegetation response to prescribed fire in a mixed conifer forest. *Canadian Journal of Forest Research*, **37**:11–22.

Matsuda, H., N. Ogita, A. Sasaki, and K. Sato. 1992. Statistical mechanics of population. *Progress of Theoretical Physics*, **88**(6):1035–1050.

Miyanishi, K. 2001. Duff consumption. In *Forest Fires-Behavior and Ecological Effects*, pp. 437–474. Academic Press, San Diego, CA.

Miyanishi, K. and E. A. Johnson. 2002. Process and patterns of duff consumption in the mixedwood boreal forest. *Canadian Journal of Forest Research*, **32**:1285–1295.

O'Brien, J. J., J. K. Hiers, R. Mitchell, J. M. Varner, and K. Mordecai. 2010. Acute physiological stress and mortality following fire in a long-unburned longleaf pine ecosystem. *Fire Ecology*, **6**(2):1–12.

Ramsey, F. 2001. *The Statistical Sleuth: A Course in Methods of Data Analysis*. Cengage Learning, 2nd ed.

Rein, G. 2009. Smoldering combustion phenomena in science and technology. *Int. Review of Chemical Engineering*, **1**:3–18.

Ryan, K. C. and W. H. Frandsen. 1991. Basal injury from smoldering fires in mature *Pinus ponderosa* Laws. *Int. J. Wildland Fire*, **1**:107–118.

Sandberg, D. 1980. Duff reduction by prescribed underburning in douglas-fir. *USDA For. Serv. Res. Paper PNW-272*.

Stauffer, H. 2008. *Contemporary Bayesian and Frequentist Statistical Research Methods for Natural Resource Scientists*. John Wiley & Sons, Inc.

Steward, F. R., S. Peter, and J. B. Richon. 1990. A method for predicting the depth of lethal heat penetration into mineral soils exposed to various fire intensities. *Canadian Journal of Forest Research*, **20**:919–926.

Swezy, D. M. and J. K. Agee. 1991. Prescribed-fire effects on fine-root and tree mortality in old-growth ponderosa pine. *Canadian Journal of Forest Research*, **21**:626–634.

Varner, J. M., D. R. Gordon, F. E. Putz, and J. K. Hiers. 2005. Restoring fire to long-unburned *pinus palustris* ecosystems: Novel fire effects and consequences for long-unburned ecosystems. *Restoration Ecology*, **13**(3):536–544.

Varner, J. M., J. K. Hiers, R. D. Ottmar, D. R. Gordon, F. E. Putz, and D. D. Wade. 2007. Overstory tree mortality resulting from re-introducing fire to long-unburned longleaf pine forests: the importance of duff moisture. *Canadian Journal of Forest Research*, **258**(11):1349–1358.

Varner, J. M., F. E. Putz, J. J. O'Brien, J. K. Hiers, R. J. Mitchell, and D. R. Gordon. 2009. Post-fire tree stress and growth following smoldering duff fires. *Forest Ecology and Management*, **11**:2467–2474.

Zeleznik, J. and D. Dickmann. 2004. Effects of high temperatures on fine roots of mature red pine (*pinus resinosa*) trees. *Forest Ecology and Management*, **199**:395–409.

APPENDIX A

Spatial Analysis at Different Scales

The scale of the model necessarily has to be finer than the scale of the field data collected for this study so that the computer model could run stably. To examine how these methods compare at different scales, a few data sets were selected that reflect particular common patters (e.g., high consumption, low consumption, edge consumption, and clustered consumption) and rescaled to $10\times$ finer their original scale. These spatial methods were then applied and compared at both scales.

Plots 7, 16, 19, 30, 34 were rescaled to $10\times$ finer than their original scale. The spatial analysis by region gave identical results at both scales, while the spatial analysis using pairs gave slightly different results at the different scales (see Table 14). When the plots were rescaled the proportion of ub pairs were reduced since the number of uu and bb pairs became more numerous within locations that were burned (see Figure 14). Since the ub pairs are the edges of the burns, it reduced linearly to approximately 1/10th its original size, whereas the uu and bb pairs grew in proportion to their area. In every case the test for clustering using the aggregation of pairs agreed between scales.

Scale	1×				10×			
Plot	UU	UB	BB	p-val	UU	UB	BB	p-val
7	0.21	0.39	0.40	0.09	0.38	0.03	0.58	0.11
16	0.75	0.20	0.05	**0.04**	0.83	0.02	0.15	**0.05**
19	0.75	0.24	0.01	0.36	0.87	0.02	0.11	0.31
30	0.58	0.26	0.16	<**0.01**	0.69	0.02	0.29	<**0.01**
34	0.44	0.49	0.07	0.24	0.66	0.04	0.30	0.32

Table 5: Data from the given plots are rescaled to ten times finer than their original scale. The UU, UB, and BB pairs are reported as well as the p-value for the permutation test that tests for clustering. A p-value less or equal than 0.05 indicates significant clustering within the plot.

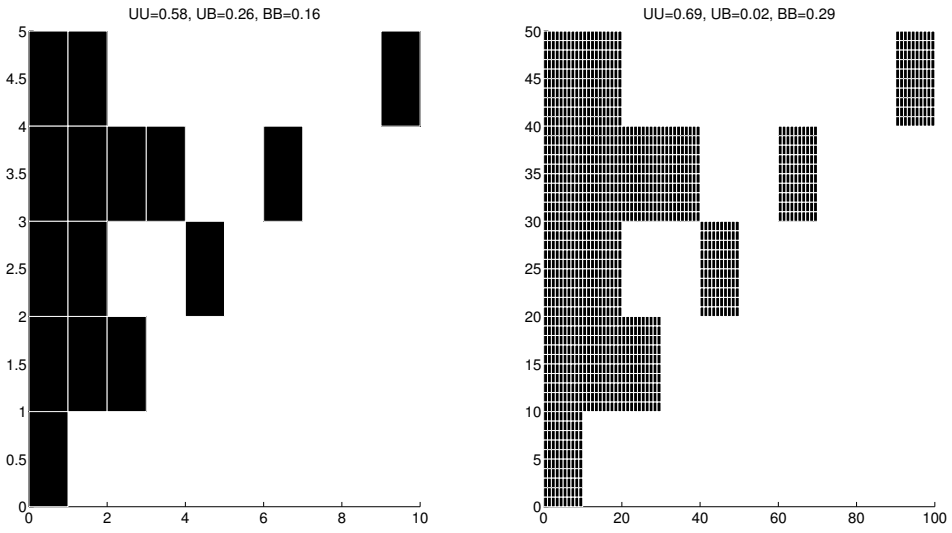

Figure 14: The spatial pattern from Plot 30 is rescaled to 10× finer than its original scale, and the proportion of the pair types UU, UB, and BB are reported.

APPENDIX B

This appendix contains binary (burn/no-burn) data from the field data at both the 0% and 5% thresholds described in the methods.

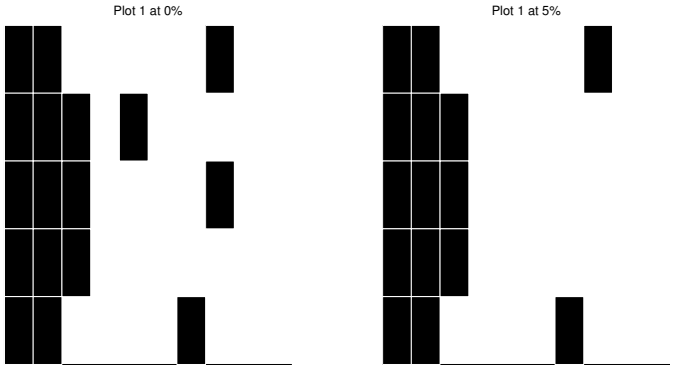

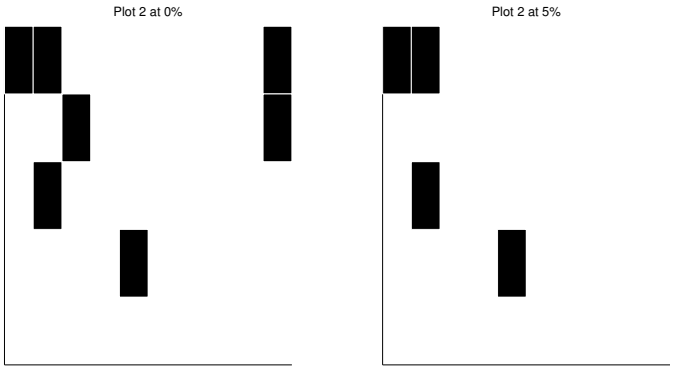

Plot 4 at 0%

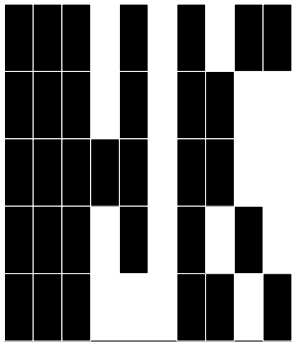

Plot 4 at 5%

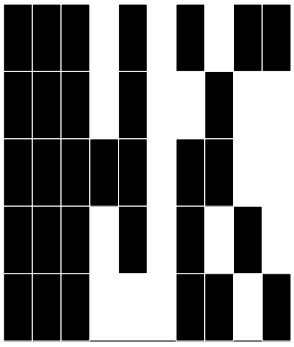

Plot 5 at 0%

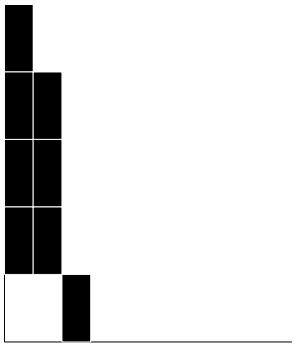

Plot 5 at 5%

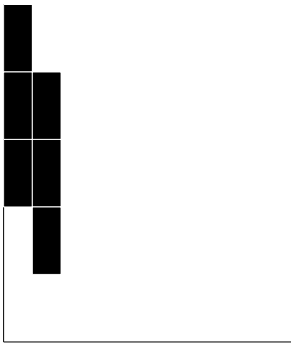

Plot 6 at 0%

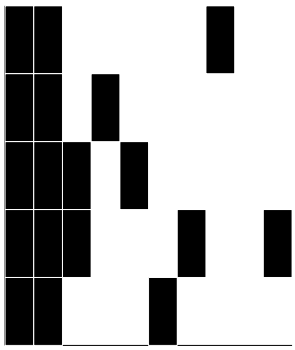

Plot 6 at 5%

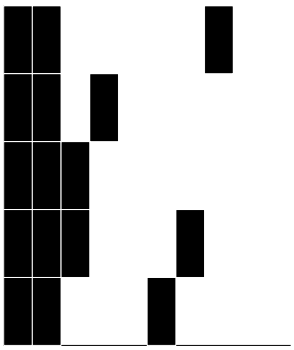

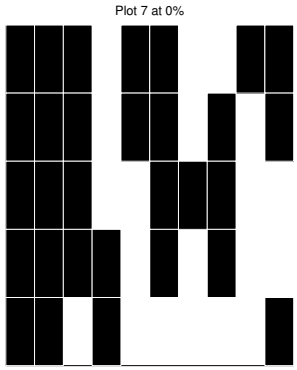
Plot 7 at 0%

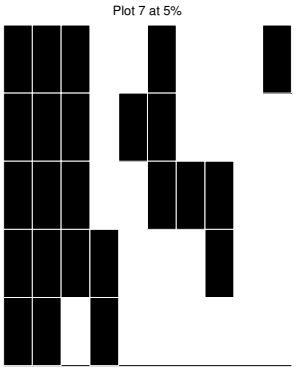
Plot 7 at 5%

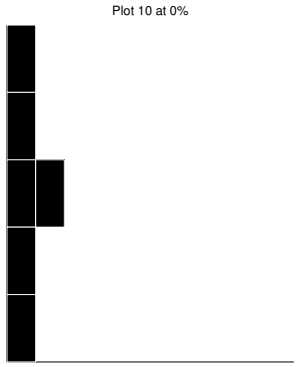
Plot 10 at 0%

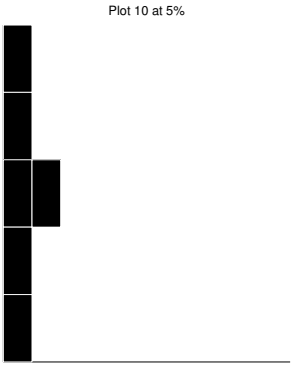
Plot 10 at 5%

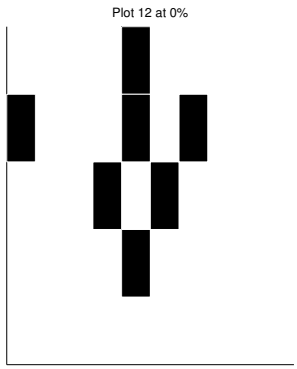
Plot 12 at 0%

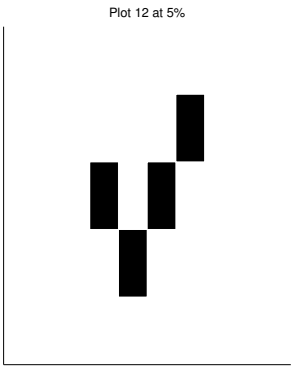
Plot 12 at 5%

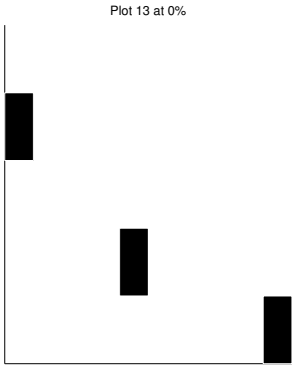
Plot 13 at 0%

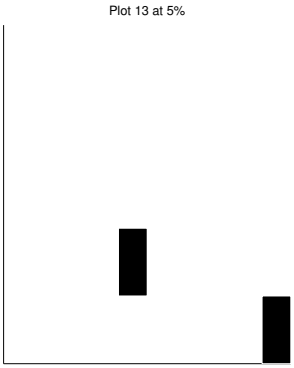
Plot 13 at 5%

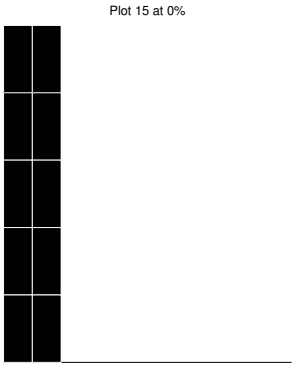
Plot 15 at 0%

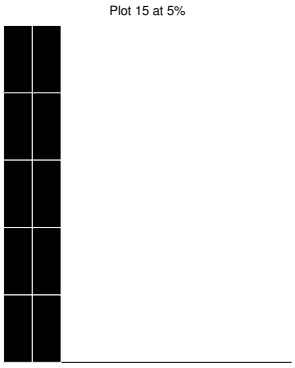
Plot 15 at 5%

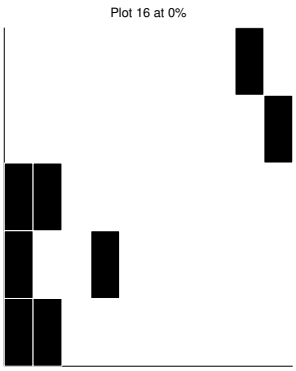
Plot 16 at 0%

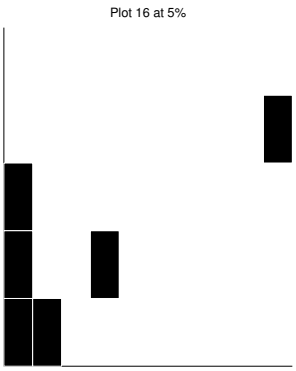
Plot 16 at 5%

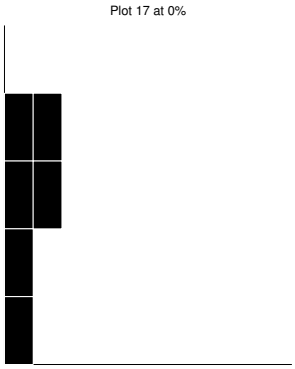
Plot 17 at 0%

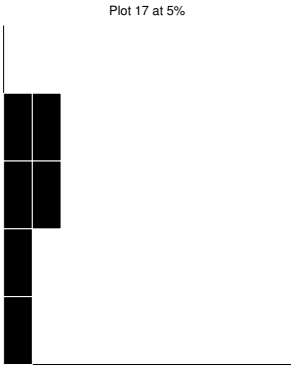
Plot 17 at 5%

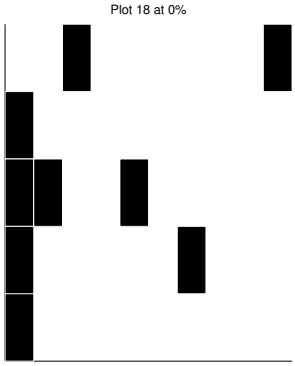
Plot 18 at 0%

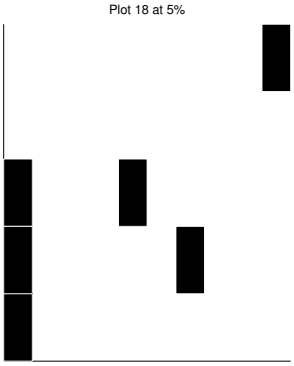
Plot 18 at 5%

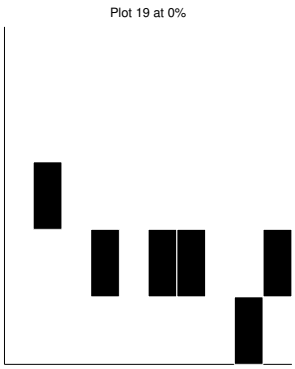
Plot 19 at 0%

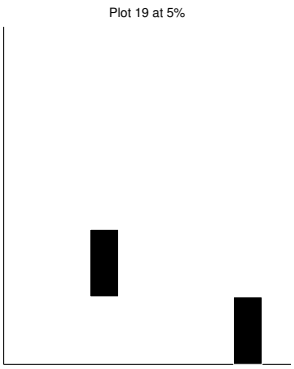
Plot 19 at 5%

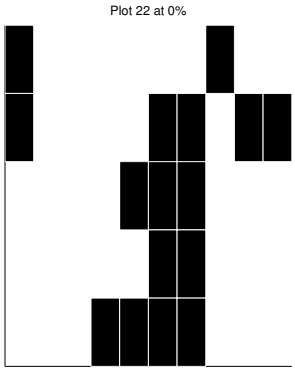
Plot 22 at 0%

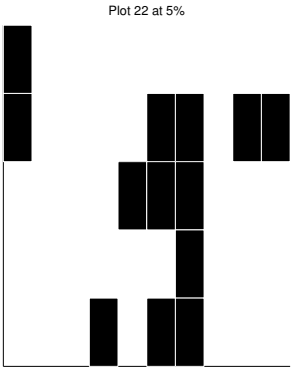
Plot 22 at 5%

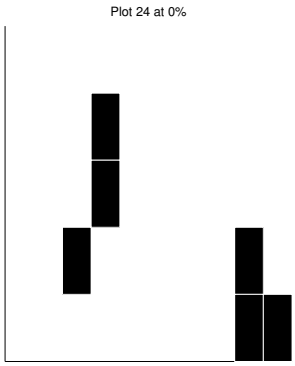
Plot 24 at 0%

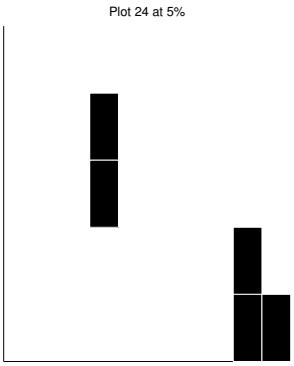
Plot 24 at 5%

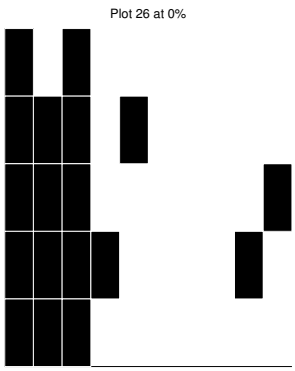
Plot 26 at 0%

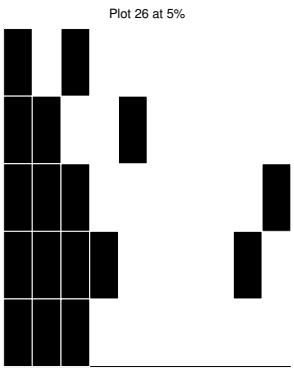
Plot 26 at 5%

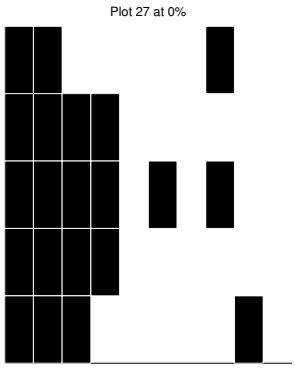
Plot 27 at 0%

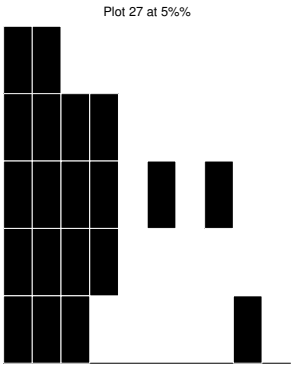
Plot 27 at 5%%

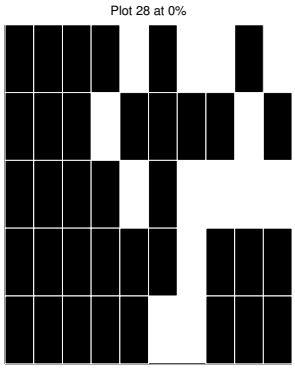
Plot 28 at 0%

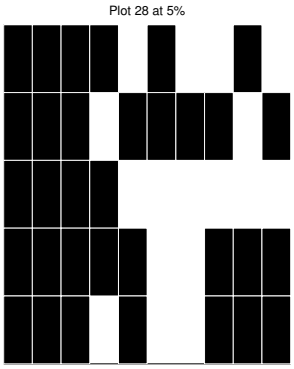
Plot 28 at 5%

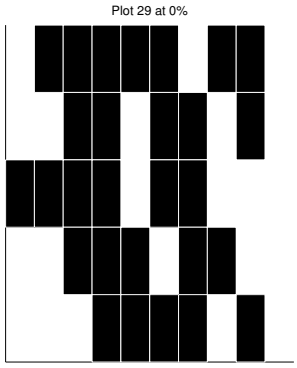
Plot 29 at 0%

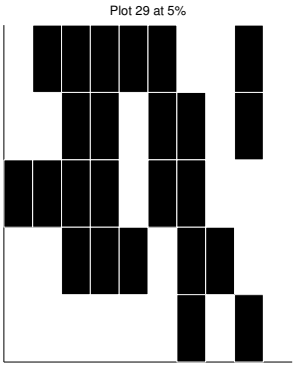
Plot 29 at 5%

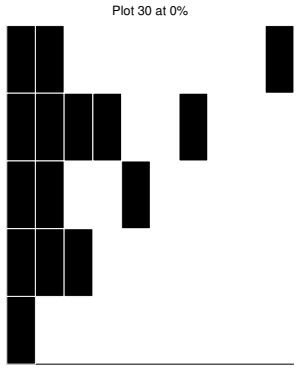
Plot 30 at 0%

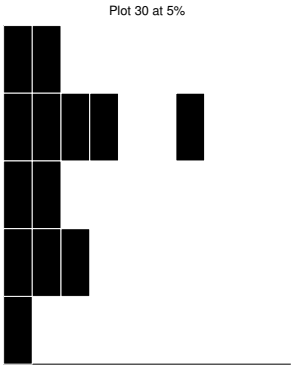
Plot 30 at 5%

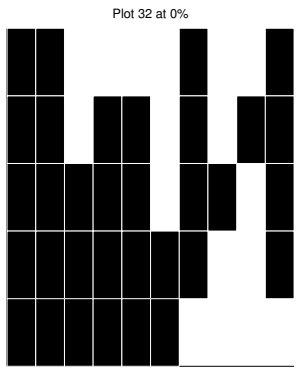
Plot 32 at 0%

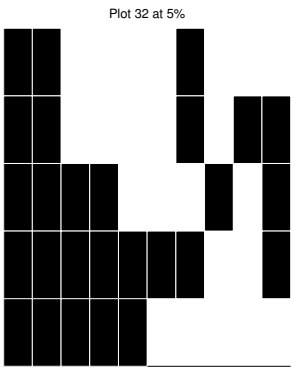
Plot 32 at 5%

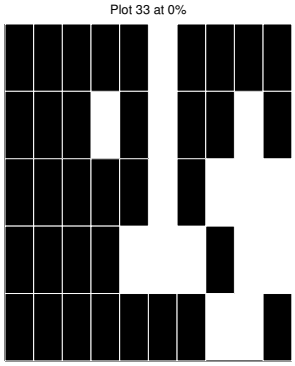
Plot 33 at 0%

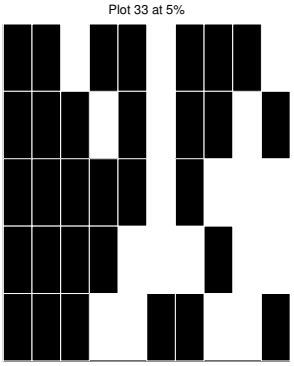
Plot 33 at 5%

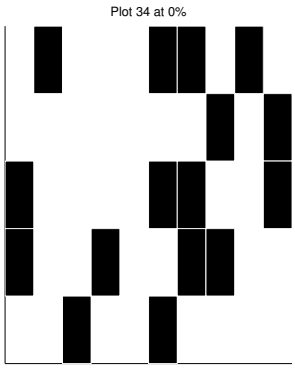
Plot 34 at 0%

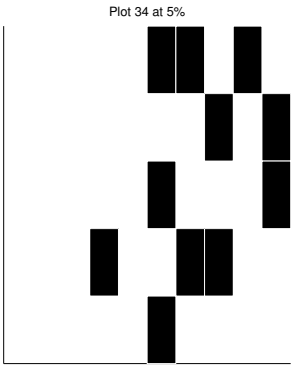
Plot 34 at 5%